Foldamer Catalysts | Hot Paper

DOI: 10.1002/ange.201400945

Building Proficient Enzymes with Foldamer Prostheses**

*Clemens Mayer, Manuel M. Müller, Samuel H. Gellman, and Donald Hilvert**

Abstract: *Foldamers are non-natural oligomers that adopt stable conformations reminiscent of those found in proteins. To evaluate the potential of foldameric subunits for catalysis, semisynthetic enzymes containing foldamer fragments constructed from α- and β-amino acid residues were designed and characterized. Systematic variation of the α→β substitution pattern and types of β-residue afforded highly proficient hybrid catalysts, thus demonstrating the feasibility of expanding the enzyme-engineering toolkit with non-natural backbones.*

The folding of linear, sequence-specific polypeptides into well-defined structures endows proteins with remarkably diverse molecular functions.[1] Chemists and biologists have long sought to mimic protein properties with non-natural oligomers.[2] Such molecules, often referred to as "foldamers", contain building blocks other than the canonical α-amino acid residues, arranged in sequences that enable them to adopt distinct conformations. Oligomers based on backbone units derived from β-amino acids, γ-amino acids, aromatic amino acids, N-substituted glycines, and other unnatural subunits can all fold into structures that resemble those found in proteins.[3] Foldamer structures have been exploited to achieve biomimetic functions including self-assembly,[4] protein recognition,[5] cell entry and lysis,[6] and even catalysis.[7] However, the few catalytic foldamers reported to date, developed through bottom-up strategies, have lacked well-defined binding pockets, thus limiting their proficiency and selectivity. A top-down approach in which non-natural oligomer segments are evaluated within an enzymatically competent polypeptide scaffold is a potentially more effective strategy for revealing design criteria that would facilitate the de novo design of active sites.

Introducing β-amino acid pairs into a short turn segment of RNase A[8] or swapping an amphiphilic α-helix for a β-peptide surrogate in a chemokine[9] yielded fully functional variants. However, introducing a larger number of artificial building blocks into RNase A reduced activity to below 1% of that of the wild-type enzyme.[10] In order to incorporate multiple β residues into a subunit crucial for catalysis, we envisioned exploiting the remarkable tolerance of helical segments to α→β substitution.[11] Such "α/β-peptides", if properly designed, can serve as potent inhibitors of protein–protein interactions that depend on α-helix recognition,[11] thus indicating that the native helical conformation is not severely distorted upon the introduction of the non-natural backbone units. In this work, we utilized the emerging principles of α-helix mimicry with α/β-peptides to design foldamer prostheses that complement an otherwise inactive protein fragment and, as a result, create highly efficient hybrid enzymes.

An engineered heterodimeric chorismate mutase (CM),[12] which catalyzes the sigmatropic rearrangement of chorismate to prephenate (hdCM; Figure 1a), served as the protein scaffold for the assembly of hybrid enzymes. hdCM was originally constructed by dissecting the helical-bundle CM from *Methanocaldococcus jannaschii* into a short N-

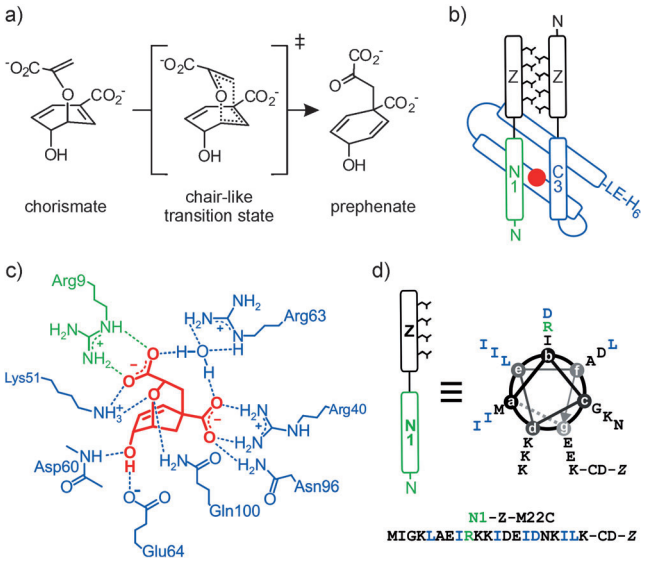

Figure 1. A heterodimeric CM as a scaffold for constructing hybrid enzymes. a) The [3,3]-sigmatropic rearrangement of chorismate to prephenate proceeds via a polarized, chair-like transition state.[20] b) A schematic representation of hdCM, which consists of a 3-helix domain (C3, blue), a one-helix segment (N1, green), and an antiparallel leucine zipper (black); the red dot shows the location of the active site. c) A schematic view of the hdCM active site with bound transition state analogue (red) and polar contact residues from N1 (green) and C3 (blue). d) A sequence and helical wheel representation of N1-Z-M22C: the catalytic Arg9 is shown in green, residues at the helical interface in blue.

[*] Prof. Dr. S. H. Gellman
Department of Chemistry, University of Wisconsin Madison
1101 University Avenue, Madison, WI 53706 (USA)
C. Mayer, Dr. M. M. Müller, Prof. Dr. D. Hilvert
Laboratory of Organic Chemistry, ETH Zürich
Hönggerberg HCI F339, 8093 Zürich (Switzerland)
E-mail: hilvert@org.chem.ethz.ch

[**] Generous support by the Schweizerischer Nationalfonds (D.H.), the National Science Foundation (CHE-1307365, S.H.G.), Novartis Pharma AG for a Novartis Graduate Fellowship (C.M.), and the Stipendienfonds der Schweizerischen Chemischen Industrie (M.M.M.) is gratefully acknowledged. We thank Raoul Rosenthal for carrying out preliminary experiments, Dr. Takashi Misawa for providing the APC building block, and Hajo Kries for helpful discussions.

Supporting information for this article (including experimental details) is available on the WWW under http://dx.doi.org/10.1002/anie.201400945.

terminal helix (residues 1–21, N1) and a 3-helix segment (residues 22–93, C3) and attaching complementary components of an antiparallel leucine zipper[13] to the individual fragments (thereby yielding N1-Z and Z-C3; Figure 1b). Both engineered fragments are inactive but the split enzyme assembles spontaneously from these fragments and catalyzes the CM reaction with a proficiency similar to that of the parent homodimeric enzyme. Unlike other split enzymes,[14] hdCM combines a unique set of desirable traits for the construction of foldamer-containing catalysts. The 52-residue one-helix fragment N1-Z is readily accessible by synthesis, thus facilitating the introduction of β residues into the N-terminal helix. A methionine-to-cysteine mutation in the linker sequence of N1-Z enables the modular attachment of different N1 analogues to the invariant leucine zipper segment by native chemical ligation (Figure S1 in the Supporting Information).[15] Furthermore, all key interactions at the quaternary interface of hdCM are made by side chains, which raises the prospect that backbone modifications will be tolerated. Finally, the active site of hdCM is formed jointly by both fragments (Figure 1c). In the active complex, N1-Z provides not only hydrophobic interactions that ensure tight packing within the four-helix bundle of hdCM but also the catalytically essential side chain of Arg9 (Figure 1d). Consequently, enzymatic activity offers a sensitive read-out of the ability of foldamer-containing N1-Z variants to mimic N1-Z itself.

We designed foldamer prostheses for hdCM by systematically introducing $\alpha\rightarrow\beta^3$ substitutions into the N-terminal helix, thereby yielding seven α/β-peptides that differ in the number, location, and/or type of β^3 residues placed within N1-Z (Figure 2a). β^3-Homoamino acids have the same side chain as the homologous α-amino acids but possess an extra CH_2 unit in the backbone (Figure 2b). Foldamer **1** contains a single $\alpha\rightarrow\beta^3$ substitution at the catalytically crucial Arg9 to assess whether a side chain projecting from the artificial backbone unit can participate in catalysis. Foldamers **2** and **3** are based on an ααβαααβ backbone repeat unit, which matches the heptad repeat pattern associated with α-helix-forming peptide segments. In **2** and **3**, the five $\alpha\rightarrow\beta$ substitutions are clustered at the solvent-exposed face of the helix formed by N1. This β-residue placement should minimize perturbations of side chains at the helical interface or the active site. The β-residue side chains in **2** mirror those of the original α residues. By contrast, **3** contains helix-stabilizing cyclic β-amino acid residues (Figure 2b)[11] to probe whether rigidifying the helix is beneficial for complex formation and catalysis. Foldamers **4**–**7** feature four possible permutations of the $\alpha\alpha\alpha\beta^3$ repeat pattern. Because this pattern does not match the heptad periodicity of the α-helix, the five β^3-amino acids spiral around the helix periphery. We surmised that the impact of the backbone modifications would be least severe in **4** and most dramatic in **7** given the number of interfacial sites with $\alpha\rightarrow\beta^3$ substitutions. The substitutions in **4** are located predominantly on the solvent-exposed face of the N-terminal helix, while **5** and **6** harbor two and four substitutions, respectively, at sites important for quaternary hydrophobic packing. In **7**, $\alpha\rightarrow\beta^3$ substitutions occur at the catalytic arginine and at critical sites for quaternary structure formation.

Foldameric prostheses were prepared by solid-phase peptide synthesis (see the Supporting Information, Figures S1–S3), and their effectiveness at supporting catalysis of the CM reaction was evaluated in the presence of recombinantly produced Z-C3. Reference values are provided by the catalytic parameters of the parent heterodimer, which

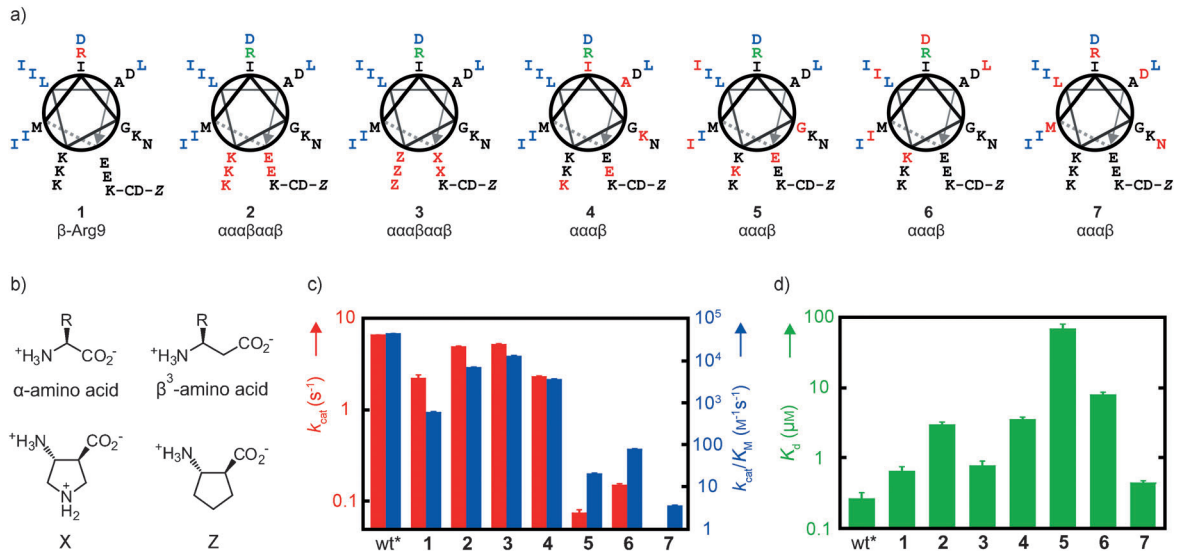

Figure 2. Design and characterization of chimeric CM enzymes. a) Foldameric N1-Z variants: the β residues are shown in red, the catalytic Arg9 in green (unless β), and residues at the helical interface in blue. b) α and β^3-homoamino acids and the structures of the cyclic building blocks used in **3**: (3*S*,4*R*)-*trans*-4-aminopyrrolidine-3-carboxylic acid (X) and (*S*,*S*)-*trans*-2-aminocyclopentane-carboxylic acid (Z). c) A comparison of the observed turnover numbers (k_{cat}, red) and apparent second-order rate constants (k_{cat}/K_m, blue) of hybrid CMs. N1-Z-M22C is designated as wt*, and no k_{cat} value was determined for **7** since this foldamer did not display saturation kinetics. d) A comparison of the dissociation constants (K_d) for the N1-Z variants with Z-C3.

displays wild-type-like activity (N1-Z-M22C, $k_{cat} = 6.7\ s^{-1}$, $K_m = 150\ \mu M$, and $k_{cat}/K_m = 44\,600\ M^{-1}s^{-1}$), and N1-Z-R9A ($k_{cat}/K_m = 1.5\ M^{-1}s^{-1}$), a variant that highlights the importance of Arg9 for catalysis and serves as a negative control; the latter variant does not show saturation kinetics. Upon mixing the synthetic N1-Z variants with Z-C3, we observed apparent second-order rate constants (k_{cat}/K_m) for chorismate consumption that span four orders of magnitude, depending on the sites of $\alpha \rightarrow \beta$ substitution (Figure 2c, Table 1, and Figure S4).

Table 1: Steady-state parameters of the hdCMs.

N1-Z fragment	k_{cat} [s^{-1}]	K_m [μM]	k_{cat}/K_m [$M^{-1}s^{-1}$]	K_d [μM]
N1-Z-M22C	6.7 ± 0.03	150 ± 2	44 600 ± 700	0.26 ± 0.06
1	2.2 ± 0.2	3800 ± 500	580 ± 30	0.64 ± 0.11
2	5.0 ± 0.1	720 ± 40	6900 ± 300	2.9 ± 0.3
3	5.2 ± 0.1	410 ± 30	13 000 ± 800	0.76 ± 0.13
4	2.3 ± 0.1	650 ± 40	3600 ± 200	3.5 ± 0.3
5	0.07 ± 0.01	3700 ± 470	20 ± 1	70 ± 12[b]
6	0.15 ± 0.01	2000 ± 150	76 ± 4	7.9 ± 0.8[b]
7[a]	–	–	3.4 ± 0.2	0.43 ± 0.04[b]
N1-Z-R9A[a]	–	–	1.5 ± 0.3	n.d.

[a] N1-Z-R9A and **7** did not show saturation kinetics. [b] K_d values were determined by measuring the inhibition of the formation of a catalytically active complex between Z-C3 and the complementary N1-Z variant **2**. n.d. = not determined.

Surprisingly, the isolated $\alpha \rightarrow \beta^3$ substitution at Arg9 (**1**) has a modest effect on k_{cat}; the k_{cat} value of 2.2 s^{-1} is only 3-fold smaller than the k_{cat} value for the parent heterodimer. However, the K_m value (3800 μM) is 25-fold higher than that for the original construct, thus suggesting an energetic penalty for orienting the β^3-hArg side chain in a manner favorable for binding the enol pyruvate carboxylate of the substrate and the transition state. The segregation of β residues away from the helical interface and active site in **2** and **3** afforded highly efficient hybrid enzymes. Turnover numbers for these variants (5.0 s^{-1} and 5.2 s^{-1}, respectively) rival the k_{cat} value obtained for the parent enzyme (6.7 s^{-1}), and the k_{cat}/K_m values for **2** and **3** are within one order of magnitude of those of natural CM enzymes.[16,17] All four designs in the $\alpha\alpha\alpha\beta^3$ series also catalyze the CM reaction, albeit with a large range of activity. Changes distal to the active site and the helical interface are well-tolerated (**4**, $k_{cat} = 2.3\ s^{-1}$, $k_{cat}/K_m = 3600\ M^{-1}s^{-1}$), but substitutions within these crucial regions yield inferior catalysts. Foldamers **5** and **6**, which have altered quaternary interfaces, display catalytic proficiencies that are 2200-fold and 600-fold lower (20 and 76 $M^{-1}s^{-1}$), respectively, than that of the parent enzyme. Replacement of the catalytic arginine with β^3-hArg along with other interfacial changes drastically diminishes activity; **7** does not display saturation kinetics ($k_{cat}/K_m = 3.4\ M^{-1}s^{-1}$) and is only roughly twice as efficient as the R9A mutant.

The introduction of β^3 residues does not adversely affect the helical folding of N1-Z variants as judged by far-UV circular dichroism (CD) spectroscopy and 1D-^{1}H NMR spectroscopy (Figure S6). The varying efficiencies of the foldamer prostheses thus presumably reflect differences in 1) the stabilities of the complexes formed with Z-C3 and 2) the extent to which the orientation of the catalytically crucial arginine side chain matches that of the native enzyme. The observed k_{cat} values provide information on the orientation of the Arg side chain, while the dissociation constant (K_d) of a given foldamer reports on quaternary structure stability. We determined dissociation constants for the complexes by adding increasing amounts of the N1-Z variants to fixed concentrations of Z-C3 and measuring reaction rates. Dissociation constants for variants not sufficiently active for titration were estimated by monitoring inhibition of the formation of an active complex with **2** (Figure 2d, Table 1, and Figure S5; see the Supporting Information for details).

Substitution of Arg9 alone or simultaneous replacement of multiple interfacial residues affords foldamers that form catalytically active complexes, although the dissociation constants (640 nM for **1** and 3,500 nM for **4**) are elevated when compared to N1-Z-M22C (260 nM). As anticipated, the introduction of cyclic β residues in **3** ($K_d = 760$ nM) generates a prosthesis that displays a higher affinity for Z-C3 than does **2** (2.9 μM), which contains flexible β^3 residues. Consistent with preorganization of the N-terminal helix, **3** unfolds at higher temperatures than the parent variant or **2** (Figure S7). The K_d values for **5** and **6** (70 μM and 7.9 μM, respectively) are significantly higher than for the other N1-Z constructs, thus demonstrating that the introduction of β^3-amino acids at the helical interface severely compromises complex formation. As a result of this handicap, the performance of both prostheses is substantially underestimated in the standard kinetic assays carried out with 2 μM Z-C3 and a 5-fold excess of the one-helix fragment. Upon extrapolation, the k_{cat} values for **5** and **6** increase by a factor of 8.2 (0.60 s^{-1}) and 1.9 (0.28 s^{-1}) with respect to the initially obtained values. Surprisingly, **7** displays the most efficient complex formation ($K_d = 0.43$ μM) of all of the foldamer prostheses. In light of the low catalytic efficiency of this foldamer, it is conceivable that the side chain of Arg9 in **7** adopts a conformation that is catalytically unproductive but beneficial for heterodimer formation. In this scenario, binding energy would be gained by avoiding electrostatic repulsion between the charged guanidinium group and the highly polar CM active site (Figure 1c).

These results demonstrate the feasibility of replacing a catalytically crucial secondary structure element with an artificial surrogate to construct highly active hybrid enzyme-like catalysts. The lessons learned provide valuable guidelines for reliably introducing non-natural segments into other proteins. Backbone modifications are well-tolerated when clustered at solvent-exposed sites; in our case, this design strategy yielded highly active hybrid CMs. Preorganization with conformationally constrained building blocks further improves foldamer-protein assembly, thereby affording proficient chimeric enzymes that display activities similar to those of naturally occurring CMs.[17] By contrast, introducing non-natural subunits at multiple sites involved in a protein–protein interface or modifications at active-site residues yields inferior catalysts. Recovering activities for these imperfect prostheses will require compensatory mutations in the binding partner Z-C3.

The guidelines we have identified should facilitate the introduction of nonstandard building blocks into a wide variety of enzymatic scaffolds and thus constitute a first step toward fully unnatural catalysts. The diversity of accessible and stable foldameric secondary structures offers unprecedented opportunities for manipulating protein function.[8] When the conformational propensities of non-natural backbones are highly predictable, as is true of the α/β segments employed here, it may be possible to optimize imperfect prostheses, such as **5**–**7**, through computationally aided laboratory evolution.[18] Ultimately, catalysts that take full advantage of the unique properties of foldamers could enable the installation of novel activities not accessible with natural enzymes.

Experimental Section

Synthesis of foldameric CMs: Wild-type and foldameric N1 variants were prepared by standard Fmoc-based solid-phase peptide synthesis as C-terminal acyl hydrazides. They were ligated to the invariable CD-Z portion in a one-pot, two-step procedure as previously described.[15a] N1-Z fragments were obtained in good yield and high purity after HPLC purification (Figure S3 and Table S1 in the Supporting Information). The 115 amino acid long three-helix fragment Z-C3 was produced recombinantly in a chorismate mutase deficient *E. coli* strain, thereby excluding the possibility of contamination with endogenous enzyme.[12]

Kinetic assay: Kinetic assays were performed by measuring the consumption of chorismate spectroscopically at either 274 nm ($\varepsilon_{274} = 2630\,\text{M}^{-1}\text{cm}^{-1}$) or 310 nm ($\varepsilon_{310} = 370\,\text{M}^{-1}\text{cm}^{-1}$) according to reported procedures.[12] The average initial velocities obtained from at least three independent measurements are plotted in Figure S4.

K_d measurements: Dissociation constants for N1-Z-M22C and foldamers **1**–**4** were determined as previously described.[12] K_d values for variants **5**–**7**, which display minimal CM activity, were determined by monitoring inhibition of the formation of an active complex between Z-C3 and **2**. IC_{50} values were obtained by plotting the resulting initial velocities at fixed concentrations of **2** and Z-C3 (both 1 μM) as a function of increasing amounts of the N1-Z fragment. Dissociation constants were calculated from the observed IC_{50} values with the Cheng–Prusoff equation.[19]

Received: January 28, 2014
Published online: May 14, 2014

Keywords: β-amino acids · enzymes · foldamers · protein design · protein engineering

[1] G. A. Petsko, D. Ringe, *Protein structure and function*, New Science Press, London, UK, **2004**.
[2] a) S. H. Gellman, *Acc. Chem. Res.* **1998**, *31*, 173–180; b) D. J. Hill, M. J. Mio, R. B. Prince, T. S. Hughes, J. S. Moore, *Chem. Rev.* **2001**, *101*, 3893–4011.
[3] a) K. Kirshenbaum, A. E. Barron, R. A. Goldsmith, P. Armand, E. K. Bradley, K. T. V. Truong, K. A. Dill, F. E. Cohen, R. N. Zuckermann, *Proc. Natl. Acad. Sci. USA* **1998**, *95*, 4303–4308; b) R. P. Cheng, S. H. Gellman, W. F. DeGrado, *Chem. Rev.* **2001**, *101*, 3219–3232; c) D. Seebach, A. K. Beck, D. J. Bierbaum, *Chem. Biodiversity* **2004**, *1*, 1111–1239; d) A. D. Bautista, C. J. Craig, E. A. Harker, A. Schepartz, *Curr. Opin. Chem. Biol.* **2007**, *11*, 685–692; e) G. Guichard, I. Huc, *Chem. Commun.* **2011**, *47*, 5933–5941; f) Z. E. Reinert, G. A. Lengyel, W. S. Horne, *J. Am. Chem. Soc.* **2013**, *135*, 12528–12531.
[4] a) D. S. Daniels, E. J. Petersson, J. X. Qiu, A. Schepartz, *J. Am. Chem. Soc.* **2007**, *129*, 1532–1533; b) W. S. Horne, J. L. Price, J. L. Keck, S. H. Gellman, *J. Am. Chem. Soc.* **2007**, *129*, 4178–4179.
[5] a) J. A. Kritzer, O. M. Stephens, D. A. Guarracino, S. K. Reznik, A. Schepartz, *Bioorg. Med. Chem.* **2005**, *13*, 11–16; b) D. G. Udugamasooriya, S. P. Dineen, R. A. Brekken, T. Kodadek, *J. Am. Chem. Soc.* **2008**, *130*, 5744–5752; c) W. S. Horne, L. M. Johnson, T. J. Ketas, P. J. Klasse, M. Lu, J. P. Moore, S. H. Gellman, *Proc. Natl. Acad. Sci. USA* **2009**, *106*, 14751–14756.
[6] a) M. Rueping, Y. Mahajan, M. Sauer, D. Seebach, *ChemBioChem* **2002**, *3*, 257–259; b) N. Umezawa, M. A. Gelman, M. C. Haigis, R. T. Raines, S. H. Gellman, *J. Am. Chem. Soc.* **2002**, *124*, 368–369.
[7] a) M. M. Müller, M. A. Windsor, W. C. Pomerantz, S. H. Gellman, D. Hilvert, *Angew. Chem.* **2009**, *121*, 940–943; *Angew. Chem. Int. Ed.* **2009**, *48*, 922–925; b) G. Maayan, M. D. Ward, K. Kirshenbaum, *Proc. Natl. Acad. Sci. USA* **2009**, *106*, 13679–13684.
[8] U. Arnold, B. R. Huck, S. H. Gellman, R. T. Raines, *Protein Sci.* **2013**, *22*, 274–279.
[9] R. David, R. Gunther, L. Baurmann, T. Luhmann, D. Seebach, H. J. Hofmann, A. G. Beck-Sickinger, *J. Am. Chem. Soc.* **2008**, *130*, 15311–15317.
[10] B. C. Lee, R. N. Zuckermann, *ACS Chem. Biol.* **2011**, *6*, 1367–1374.
[11] L. M. Johnson, S. H. Gellman, *Methods Enzymol.* **2013**, *523*, 407–429.
[12] M. M. Müller, H. Kries, E. Csuhai, P. Kast, D. Hilvert, *Protein Sci.* **2010**, *19*, 1000–1010.
[13] I. Ghosh, A. D. Hamilton, L. Regan, *J. Am. Chem. Soc.* **2000**, *122*, 5658–5659.
[14] S. S. Shekhawat, I. Ghosh, *Curr. Opin. Chem. Biol.* **2011**, *15*, 789–797.
[15] a) G. M. Fang, Y. M. Li, F. Shen, Y. C. Huang, J. B. Li, Y. Lin, H. K. Cui, L. Liu, *Angew. Chem.* **2011**, *123*, 7787–7791; *Angew. Chem. Int. Ed.* **2011**, *50*, 7645–7649; b) P. E. Dawson, T. W. Muir, I. Clarklewis, S. B. H. Kent, *Science* **1994**, *266*, 776–779.
[16] S. Sasso, C. Ramakrishnan, M. Gamper, D. Hilvert, P. Kast, *FEBS J.* **2005**, *272*, 375–389.
[17] D. H. Calhoun, C. A. Bonner, W. Gu, G. Xie, R. A. Jensen, *Genome Biol.* **2001**, *2*, research0030.1-30.16.
[18] a) D. Hilvert, *Annu. Rev. Biochem.* **2013**, *82*, 447–470; b) C. Jäckel, P. Kast, D. Hilvert, *Annu. Rev. Biophys.* **2008**, *37*, 153–173.
[19] Y. Cheng, W. H. Prusoff, *Biochem. Pharmacol.* **1973**, *22*, 3099–3108.
[20] a) D. J. Gustin, P. Mattei, P. Kast, O. Wiest, L. Lee, W. W. Cleland, D. Hilvert, *J. Am. Chem. Soc.* **1999**, *121*, 1756–1757; b) S. G. Sogo, T. S. Widlanski, J. H. Hoare, C. E. Grimshaw, G. A. Berchtold, J. R. Knowles, *J. Am. Chem. Soc.* **1984**, *106*, 2701–2703.

